Int J Earth Sci (Geol Rundsch) (2003) 92:348–363
DOI 10.1007/s00531-003-0331-1

ORIGINAL PAPER

G. Han · J. Yans · M. Goudalier · F. Lacquement ·
R. M. Corfield · J. L. Mansy · F. Boulvain · A. Préat

Recognition and implication of tectonic loading-induced reheating in the northern Variscan front (Belgium and northern France), based on an illite Kübler index and oxygen isotope study

Received: 6 May 2002 / Accepted: 21 March 2003 / Published online: 4 July 2003

Abstract Illite Kübler index (KI) and oxygen isotope (brachiopods and micrites) investigations have been performed on more than 300 Frasnian limestones sampled in one borehole and numerous outcrops in the Dinant Synclinorium (Belgium, northern France) of the northern Variscan front. The illite Kübler index and $\delta^{18}O$ data of a 3-km-thick, tectonically repeated Frasnian series from the Focant borehole are compared with their surrounding surface correspondents and document in-situ reheating induced by Variscan tectonic loading, which post-dated sedimentary burial alteration. The boundary between these two thermal processes (sedimentary burial and tectonic loading) on the Focant profile corresponds to an important location where the heat induced by the tectonic loading was equivalent to that Frasnian strata suffered during maximum sedimentary burial. Mainly based on this knowledge and on a former conodont colour alteration index study, the thickness of the eroded thrust sheet in the Focant area is estimated to be around 3,000 m. Oxygen isotopic exchange in these Frasnian closed carbonate systems, occurring under highest-grade diagenesis and anchimetamorphism, records two events. Brachiopods present a quite different and more homogeneous pattern, due to their higher resistance to heat alteration. These thermal events caused both $\delta^{18}O$ records to become increasingly lighter than the presumed original seawater signature. The comparison between KI and $\delta^{18}O$ profiles indicates that illite KI analysis is more appropriate than $\delta^{18}O$ in highlighting the temperature variations in the burial metamorphism at the periphery of orogenic belts.

Keywords Focant borehole · Frasnian carbonates · Illite Kübler index · Oxygen isotopes · Sedimentary burial · Tectonic loading

G. Han
Geological Survey of Belgium,
Royal Belgian Institute of National Science, 13 rue Jenner,
1000 Brussels, Belgium

J. Yans
Service de Géologie Fondamentale et Appliquée,
Faculté Polytechnique de Mons, rue de Houdain,
7000 Mons, Belgium

M. Goudalier · J. L. Mansy
Sédimentologie et Géodynamique, UMR 8577 CNRS,
Université de Lille 1, 59655 Cédex Villeneuve d'Ascq, France

F. Lacquement
Bureau des Ressources Géol. et Min.,
3 av. Guillemin, 45060 Cédex 2 Orléans, France

R. M. Corfield
Department of Earth Sciences, University of Oxford,
Parks Road, Oxford, OXI 3PR, UK

F. Boulvain
Géologie-Pétrologie-Géochimie, Université de Liège,
B20, 4000 Sart-Tilman, Liège, Belgium

A. Préat (✉)
Département des Sciences de la Terre et de l'Environnement,
Université Libre de Bruxelles, 50 av. FD Roosevelt, CP160/02,
1050 Brussels, Belgium
e-mail: apreat@ulb.ac.be

Introduction

Very low-grade metamorphism is widely developed at the periphery of orogenic belts (Robinson and Merriman 1999). In such subgreenschist metamorphism (including strong diagenesis), illite KI studies of sedimentary rocks are important indicators (Kisch 1987). KI studies, combined with other analyses (cf. petrography, isotopes) of the geological setting, have led to a greater understanding of the distribution of metamorphic grade, style and origin. Studies have been carried out, for example, in the Glarus Alps of northeast Switzerland (Frey 1988), in the Variscan belt in southwest England (Warr et al. 1991), and in the Caledonides of eastern England and Scandinavia (Merriman et al. 1993; Warr et al. 1996). In their review of previous studies, Merriman and Frey (1999) concluded that burial has a fundamental influence on low-temperature metamorphism, no matter whether the over-

burden is generated by normal basin-filling sedimentation or by tectonostratigraphical thickening.

Compared with other factors, temperature is believed to be the most important parameter affecting the Kübler index (Kübler 1967a, 1967b, 1968). KI values of anchizone and epizone grades correlate with changes in crystallite size observed by transmission electron microscopy (Merriman et al. 1990, 1995; Nieto and Sanchez-Navas 1994). Based on mineral facies study, the illite KI zonation (Kübler 1967a), which can also be associated with coalification stage (e.g. Teichmüller et al. 1979), corresponds to recognised changes in mineral facies from zeolite, through prehnite–pumpellyite, to greenschist facies (e.g. Warr 1996). The KI method is restricted to zones of low-grade metamorphism and strong diagenesis (Kübler and Jaboyedoff 2000). Geological processes such as regional burial, tectonic overburden and local contact metamorphism are the main geological causes of such illite KI (e.g. Schaer and Persoz 1976; Fortey et al. 1993; Smellie et al. 1996). The diagenetic alteration of oxygen isotopes, which occurs during carbonate cementation, replacement and recrystallization (Marshall 1992), hinders the precise temperature determination of palaeo-oceans, but can be applied to diagenetic/metamorphic studies (e.g. Weis and Préat 1994; Machel et al. 1996; Sharp 1999). Such $\delta^{18}O$ values depend on the temperature and isotopic composition of fluids during alteration, since different carbonate minerals show slight differences in fractionation (Marshall 1992; Holser et al. 1996). The typical KI pattern caused by a thermal event could be related to various gradients, such as stratigraphical, depth and distance.

The filling of sedimentary basins and subsequent tectonic inversion is a general evolutionary process of many ancient basins (Einsele 1992; Busby and Ingersoll 1995). During its evolution, the basin fill can experience two types of thermal regimes, sedimentary burial and tectonic loading, if their burdens are significant within a steady, upward-dominated heat transfer environment. The thermal record of the former has been widely documented in our study area (Dinant Synclinorium) and stratigraphical gradients (increasing KI with stratigraphical age) established for the Late Palaeozoic (Dandois 1985; Muchez et al. 1991; Fielitz and Mansy 1999; Han et al. 2000). The record of reheating by the latter (i.e. tectonic loading) was also demonstrated (Han et al. 2000; Juch 2000), but there has been no further discussion on its origin and implication in terms of basin evolution (e.g. Dinant Synclinorium). This paper is therefore devoted to the analysis of tectonic loading by studying the deep Focant borehole (southern part of the Dinant Synclinorium) composed of more than 3,000 m of repeated Frasnian formations. Since regional stratigraphical illite KI values from Middle Devonian to Lower Carboniferous series are known (Han 1999; Han et al. 2000), the Focant borehole constitutes an ideal case study of the processes related to burial. Additional analyses of oxygen isotopes have been carried out in order to characterize the nature of burial and related palaeofluids.

The purpose of this paper is (1) to document the reheating under the Variscan tectonic loading regime, based on well-constructed depth profiles of the illite crystallinities and oxygen isotopes, and compare the KI pattern with those of the peripheries in other orogenic belts; (2) to discuss the significance of the formative mechanisms and the conditions of such reheating in order to gain a better understanding of the Variscan tectonic load; and (3) to compare the thermal behaviours of KI, conodont colour alteration index and oxygen isotopes of carbonates during diagenesis and very low-grade metamorphism.

Geological setting

The Dinant Synclinorium (southern Belgium and northern France), including the Philippeville Massif, is located in the northern part of the Ardenne allochthon, and forms part of the Rhenohercynian belt of the Mid-European Variscides (Fig. 1, inset). To the north of the Midi Fault, which represents the northern boundary of the synclinorium, lies the Brabant Massif with its parautochthonous cover (Meilliez and Mansy 1990).

The Variscan front in Belgium and northern France is represented by Brabant parautochthonous and Ardenne allochthonous massifs. Both consist of Early Palaeozoic incompetent basement composed of siliciclastic formations with Caledonian–Acadian deformations (Michot 1976; Meilliez et al. 1991; Mansy and Meilliez 1993). The subsequent Palaeozoic sedimentation on the passive margin of the Ardenne developed during Devonian times in some synsedimentary NE–SW and NW–SE fault-controlled sub-basins (Fig. 1A; Thorez et al. 1988; Kasimi and Préat 1996; Lacquement 2001). Devonian strata generally thicken by ratios of 1:3 to 1:5 from the northerly Brabant Massif towards the south. Landmasses were located in northern Belgium up until Carboniferous times, while southerly depositional centres were connected to French basins. Hence, many hiatuses occur in the Brabant area that are missing in the Ardenne (Mamet and Préat 1996). Extensional tectonics occurred close to the Rocroi Massif, as indicated by middle to late Devonian intrusion of granodiorite dykes, and was subsequently followed by regional low-grade metamorphism (Goffette et al. 1991). At the beginning of late Carboniferous times, a series of non-marine to paralic siliciclastic sediments (Bless 1983; Paproth et al. 1994) were deposited in a foreland basin setting (Bless et al. 1989; Meilliez et al. 1991), with a maximum thickness estimated to 4,500 m in the central part of the synclinorium, based on a conodont colour alteration index (CAI) study (Helsen 1995a).

The Variscan northward thrusting was activated along the former, steep extensional fault planes and new, subhorizontal, lithologically weak planes (Bless et al. 1989; Meilliez and Mansy 1990). The shutdown of sedimentation within the Dinant Synclinorium, caused by the thrusting during Silesian times, is characterized by a gradual northward migration (K/Ar dating, Piqué et al.

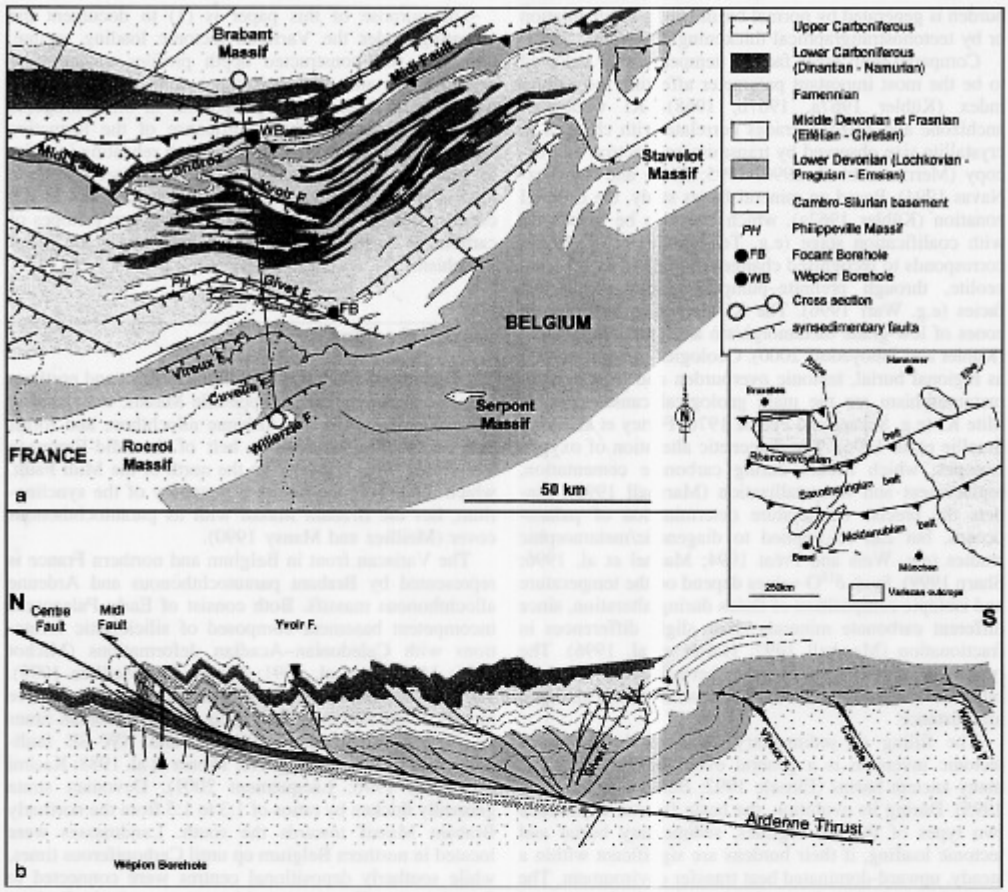

Fig. 1 **a** Geological map of southern Belgium and northern France with location of the Dinant Synclinorium, limited to the north by the Midi Fault and to the south by the Caledonian basement of the Rocroi and Stavelot massifs. The synclinorium, with dominant NE–SW and NW–SE synsedimentary faults, shows a general ENE–WSW strike. **b** Structural cross section through the synclinorium. The inset map shows the location of the study region in the Rhenohercynian belt of the Mid-European Variscides

1984). This migration has been confirmed by the position of the diagenetic/anchizonal boundary which is systematically located in younger series in the north (Han et al. 2000). The basin shortening, estimated at a minimum of 30% (Raoult and Meilliez 1986; Adams and Vandenberghe 1993; Mansy et al. 1997), produced a tectonically thickened stack, which changed the nature of the overburden from a normal sedimentary, buried sequence to a thicker tectonic load. Following Variscan movement, the region remained a palaeohigh except for its western and eastern flanks where local, thin Meso-Cenozoic cover was deposited (Ziegler 1990; Meilliez et al. 1991).

The Frasnian series, which are the focus of this paper, consist of an alternation of shales and limestones (Boulvain and Coen-Aubert 1997; Boulvain et al. 1999). They are biostratigraphically well defined by their conodont zonation (Bultynck et al. 1998). Facies analysis reveals a generally shallow sedimentation environment (broad shelf) with carbonate mud mounds in an outer ramp setting (Fig. 2). The thickness of the Frasnian series ranges from about 450 m in the southern border and 350 m in the Philippeville Massif to 250 m in the northern border of the Dinant Synclinorium (Boulvain et al. 1999).

correlation (R^2=0.982) (Robion et al. 1999; Averbuch, personal communication).

Oxygen isotopes

A total of 180 samples were collected for oxygen isotope study of both pure micrites and brachiopod shells from limestones, shaly limestones and calcareous shales of the Focant borehole and the La Boverie quarry (Fig. 3). Thin sections (0.5 to 1 mm thick) were prepared for each brachiopod and used for optical microscope and cathodoluminescence study. From the 180 samples collected, 83 homogeneous micrites representing 91% of the total micrite samples were retained, and 53 non-luminescent brachiopods (i.e. with non-luminescent internal secondary layer) representing about 60% of the total shells. Both brachiopods and micrites were used because they are considered to be likely differential isotopic reactors during diagenetic alteration (Marshall 1992).

The oxygen isotope compositions were measured after drilling about 10 mg of powder for each considered sample with a 0.3- or 0.5-mm-thick drill. The powder was cleaned in 10% hydrogen peroxide for about 30 min to remove any organic contamination, rinsed and then dried for 30 min at 60 °C. The samples were analysed with a VG Isotech PRISM mass spectrometer in the Oxford laboratory by online reaction, with purified orthophosphoric acid at 90 °C. Oxygen isotope ratios are expressed as per mil (‰) deviation from the Peedee Belemnite (PDB) standard. Calibration to the PDB standard was performed via the laboratory standard to NOCZ. Reproducibility of replicate standards was always better than 0.1‰.

Results

Illite Kübler index

Illite KI variations in Frasnian rocks of the Dinant Synclinorium

The detailed illite KI investigation of the surface strata (limestones and shales) from Middle Devonian to Lower Carboniferous series in eight subareas of the Dinant Synclinorium revealed the following characteristics (Han et al. 2000): (1) 63% of total illite KI values fall into the highest-grade diagenetic zone (0.42–0.62° $\Delta 2\theta$), 30% in the lower anchimetamorphic zone (0.33–0.42° $\Delta 2\theta$), and 7% outside these zones; (2) a clear correlation between increasing metamorphic grade based on illite KI data and stratigraphic depth is ubiquitous; (3) the position of the diagenetic-anchizone boundary occurs at higher stratigraphic levels towards the north.

The clay assemblage of the studied Frasnian rocks (106 samples) is characterized by dominant illite and chlorite with a few smectite, kaolinite and random mixed-layers. All measured illite KI and corresponding KIS values are listed in Table 1 as a function of stratigraphical formation and geographical location. According to mean KIS values at each location, the illite KI lateral distribution of surface Frasnian strata in the Dinant Synclinorium reveals a regional difference (Fig. 3). In the southern border, illite KI averages 0.55°, with a range from 0.45 to 0.67° $\Delta 2\theta$. Illite KI averages 0.52 and 0.47° in the western and eastern parts of the Philippeville Massif respectively, and ranges from 0.41 to 0.65° and from 0.38 to 0.58° $\Delta 2\theta$. The illite KI of the northern border of the Dinant Synclinorium shows the highest grade, reaching 0.37° on average, and ranging from 0.33 to 0.41° $\Delta 2\theta$. Such a geographical distribution displays an obvious increase in metamorphic grade northwards from the diagenetic zone to the anchizone, and is consistent with the general pattern determined from the complete Middle to Upper Devonian series in the Dinant Synclinorium, including the Philippeville Massif (Han et al. 2000).

Illite KI variations in Frasnian rocks of the Focant borehole

The Focant borehole (Fig. 1A), with a depth of 3,208 m, cuts several thrust sheets with different deformational styles (Boulvain and Coen-Aubert 1997), repeating the Frasnian strata for more than 3 km (Fig. 4). The normal thickness of the Frasnian series is about 350–450 m in the southern border of the Dinant Synclinorium and in the Philippeville Massif (Fig. 2) where the stratotype has been historically defined.

Clay assemblages of the Frasnian strata from the borehole consist of illite and chlorite, taking up on average about 65 and 35% respectively (Goudalier 1998). The averages and ranges of illite KI (based on 98 samples of Table 2) from each formation (or member) in each tectonic sheet enable subdivision of the Focant profile into two main parts, the boundary lying at 1,100–1,200 m (Fig. 4). In the upper zone (zone A), KI values do not present any significant change with depth or stratigraphical formation, varying from 0.45 to 0.60° $\Delta 2\theta$, which is similar to the outcrop values of the nearby southern border (see above). In the lower section (zone B), an obvious gradient with an average slope of 0.013° $\Delta 2\theta$/100 m, based on a regression equation (Y_{KI}= 0.626–(0.124/1.000)X_{Depth}) with R^2=0.883 (using mean KI and depth of formation section on regression plots of Statview 4.0), is present independently of the stratigraphy. The maximum illite KI difference in the same formation between these two zones reaches 0.25° $\Delta 2\theta$ (much larger than a complete anchizone interval), based on mean comparison between the lowermost Neuville Formation (zone B) and its correspondent in the upper section (zone A).

$\delta^{18}O$ variations in Frasnian rocks of the Focant borehole and La Boverie quarry

The large La Boverie quarry exposes superimposed Arche (*transitans-punctata* conodont zones) and Lion (*hassi to jamieae* conodont zones) members which constitute two of the three Frasnian carbonate mound stratigraphical levels in Belgium, each mound being embedded by shales and argillaceous limestones (Boulvain et al. 1999). The oxygen isotopic investigation displays no significant difference between these members in the quarry. The brachiopod $\delta^{18}O$ values range from −4.647 to −8.380‰,

Table 1 Illite Kübler indices of Frasnian beds in the Dinant Synclinorium and Philippeville Massif. *KI (Lille)* Illite Kübler index (°Δ2θ) before calibration, *KIS* Kübler index standard

Sample no.	Site	Formation (member)	KI (Lille)	KI (KIS)	Sample no.	Site	Formation (member)	KI (Lille)	KI (KIS)
SBDS					H48a[a]	Franchimont	NEU-VAL	0.40	0.6
H18	Foisches	BIE	0.38	0.57	H48b[a]	Franchimont	NEU-VAL	0.40	0.6
H18a	Foisches	BIE	0.35	0.52	H51	V.Gambon	PHV	0.35	0.52
H18b	Foisches	BIE	0.34	0.5	H51a	V.Gambon	PHV	0.36	0.52
H18c	Foisches	BIE	0.44	0.67	H51b	V.Gambon	PHV	0.35	0.52
H18d	Foisches	BIE	0.40	0.6	H51c	V.Gambon	PHV	0.31	0.45
H19	Foisches	NEU-VAL	0.35	0.52	H53a	V.Gambon	PHV	0.31	0.45
H19a	Foisches	NEU-VAL	0.38	0.57	H52a	V.Gambon	NEU-VAL	0.40	0.6
H19b[a]	Foisches	NEU-VAL	0.40	0.6	H54	Sautour	PDF	0.38	0.57
H20[a]	Foisches	NEU-VAL	0.38	0.57	H54a	Sautour	PDF	0.37	0.55
H32	Gimnée	CHA	0.35	0.52	H54b	Sautour	PDF	0.31	0.45
H32a	Gimnée	CHA	0.35	0.52	H54c	Sautour	PDF	0.37	0.55
H32b	Gimnée	CHA	0.31	0.45	H55	Sautour	PHV	0.38	0.57
H32c	Gimnée	CHA	0.31	0.45	H55a	Sautour	PHV	0.40	0.6
H33	Gimnée	BIE	0.40	0.6	H55b	Sautour	PHV	0.42	0.64
H33a[a]	Gimnée	BIE	0.39	0.58	H56	Sautour	PHV	0.29	0.41
H33b[a]	Gimnée	BIE	0.38	0.57	H57	Sautour	NEU-VAL	0.42	0.64
H33c	Gimnée	BIE	0.35	0.52	H57a	Sautour	NEU-VAL	0.35	0.52
ePHM					CF21	Cerfontaine	PHV	0.32	0.46
H36	Soulme	CHA	0.33	0.48	CF28	Cerfontaine	PHV	0.31	0.45
H39	Soulme	NIS	0.31	0.45	CF29	Cerfontaine	PHV	0.32	0.46
H39a	Soulme	NIS	0.33	0.48	CF35	Cerfontaine	PHV	0.35	0.52
H40a	Soulme	BIE	0.27	0.38	CF38	Cerfontaine	PHV	0.36	0.53
H41[a]	Soulme	NEU-VAL	0.29	0.41	CF75	Cerfontaine	PHV	0.38	0.57
H41a[a]	Soulme	NEU-VAL	0.29	0.41	CF76	Cerfontaine	PHV	0.38	0.57
H41b	Soulme	NEU-VAL	0.28	0.39	CF76bis	Cerfontaine	PHV	0.43	0.65
H41c	Soulme	NEU-VAL	0.29	0.41	CF78	Cerfontaine	PHV	0.29	0.41
H42	Soulme	NEU-VAL	0.30	0.43	CF79	Cerfontaine	PHV	0.39	0.58
H42a[a]	Soulme	NEU-VAL	0.31	0.45	CF83	Cerfontaine	PHV	0.41	0.62
MAR202	Marmont	CHA	0.31	0.45	CF122	Cerfontaine	PHV	0.31	0.45
MAR209	Marmont	CHA	0.32	0.46	CF40[a]	Cerfontaine	PHV	0.35	0.52
MAR210	Marmont	CHA	0.30	0.43	CF115[a]	Cerfontaine	PHV	0.41	0.62
MAR212	Marmont	CHA	0.33	0.48	SZ1	Beauchateau	NEU	0.38	0.57
MAR217	Marmont	CHA	0.30	0.43	SZ2	Beauchateau	NEU	0.40	0.6
MAR219	Marmont	CHA	0.30	0.43	SZ3	Beauchateau	NEU	0.34	0.5
MAR001	Marmont	BIE	0.30	0.43	SZ4[a]	Beauchateau	VAL	0.38	0.57
MAR020	Marmont	BIE	0.32	0.46	NBDS				
MAR042	Marmont	BIE	0.35	0.52	PRY80	Pry	PHV	0.26	0.36
MAR062	Marmont	BIE	0.34	0.5	PRY69	Pry	PHV	0.24	0.33
MAR103	Marmont	BIE	0.31	0.45	PRY64[a]	Pry	PHV	0.26	0.36
MAR111	Marmont	BIE	0.32	0.46	PRY63	Pry	PHV	0.26	0.36
V2[a]	Hautmont	NEU	0.39	0.58	PRY48	Pry	PHV	0.26	0.36
V3	Hautmont	NEU	0.33	0.48	PRY47	Pry	PHV	0.28	0.39
V4	Hautmont	NEU	0.34	0.5	PRY42	Pry	PHV	0.26	0.36
V9[a]	Hautmont	NEU	0.38	0.57	PRY28	Pry	PHV	0.27	0.38
V15	Hautmont	NEU	0.39	0.58	PRY27	Pry	PHV	0.27	0.38
V14[c]	Hautmont	VAL	0.36	0.53	PRY26	Pry	PHV	0.27	0.38
wPHM					GO128	Gourdinne	PHV	0.29	0.41
H45	Franchimont	NIS	0.35	0.52	GO160	Gourdinne	PHV	0.24	0.33
H46	Franchimont	CHA	0.33	0.48	GO202	Gourdinne	PHV	0.24	0.33
H46a	Franchimont	CHA	0.31	0.45	GO240	Gourdinne	PHV	0.24	0.33
H47	Franchimont	BIE	0.32	0.46	GO283	Gourdinne	PHV	0.25	0.34
H47b	Franchimont	BIE	0.38	0.57	GO301	Gourdinne	PHV	0.25	0.34
H47c	Franchimont	BIE	0.31	0.45	GO320	Gourdinne	PHV	0.26	0.36
H48[a]	Franchimont	NEU-VAL	0.38	0.57	GO327	Gourdinne	PHV	0.29	0.41

[a] The lithology of these samples is shaly limestone (or calcareous shale), others are limestones. V.Gambon, Villers-le-Gambon; SBDS, southern border of Dinant Synclinorium; wPHM, western part of Philippeville Massif; ePHM, eastern part of Philippeville Massif; NBDS, northern border of Dinant Synclinorium. Formation and member names are NIS, Nismes Formation; CHA (PDF), Châlon (Pont de la Folle) Formation; BIE, Bieumont Member; PHV, Philippeville Formation; NEU (VAL), Neuville (Valisettes) Formation (after Boulvain et al. 1993, 1999)

Table 2 Illite Kübler indices of the Focant borehole

Depth (m)	Stage	Formation (member)	KI (Lille)[a]	KI (KIS)	Depth (m)	Stage	Formation (member)	KI (Lille)	KI (KIS)
7.4	Fam	FAME	0.35	0.52	1,501	Fra	NEU	0.325	0.48
7.4	Fam	FAME	0.4	0.60	1,549	Fra	BOU	0.275	0.39
50.5	Fam	FAME	0.375	0.56	1,549	Fra	BOU	0.275	0.39
99	Fra	NEU	0.35	0.52	1,600	Fra	NEU[b]	0.275	0.39
124.3	Fra	NEU	0.375	0.56	1,649	Fra	BIE	0.325	0.48
152	Fra	NEU	0.4	0.60	1,652	Fra	BIE	0.27	0.38
152	Fra	NEU	0.4	0.60	1,700	Fra	BIE	0.25	0.35
175	Fra	NEU	0.35	0.52	1,748	Fra	BOU	0.25	0.35
201	Fra	NEU	0.35	0.52	1,800	Fra	BOU	0.275	0.39
255	Fra	NEU	0.375	0.56	1,800	Fra	BOU	0.25	0.35
277	Fra	NEU	0.4	0.60	1,851	Fra	NEU[b]	0.25	0.35
298	Fra	MAT	0.375	0.56	1,901	Fra	BOU	0.25	0.35
305	Fra	MAT	0.35	0.52	1,957	Fra	BOU	0.275	0.39
326	Fra	MAT	0.4	0.60	1,957	Fra	BOU	0.25	0.35
351	Fra	MAT	0.3	0.44	2,000	Fra	NEU	0.25	0.35
395	Fra	NEU	0.4	0.60	2,049	Fra	NEU	0.275	0.39
454.5	Fra	MAT	0.35	0.52	2,104	Fra	BOU	0.25	0.35
451	Fra	MAT	0.35	0.52	2,104	Fra	BOU	0.25	0.35
501	Fra	MAT	0.35	0.52	2,153	Fra	BOU	0.225	0.31
548	Fra	MAT	0.375	0.56	2,200	Fra	BIE	0.275	0.39
601	Fam	FAME	0.35	0.52	2,252	Fra	BIE	0.225	0.31
601	Fam	FAME	0.35	0.52	2,252	Fra	BIE	0.25	0.35
650	Fam	FAME	0.35	0.52	2,302	Fra	BOU	0.25	0.35
702	Fra	MAT	0.375	0.56	2,350	Fra	BOU	0.25	0.35
750.4	Fra	MAT	0.375	0.56	2,400	Fra	BIE	0.225	0.31
750.4	Fra	MAT	0.35	0.52	2,400	Fra	BIE	0.25	0.35
800	Fra	MAT	0.325	0.48	2,452	Fra	ERM	0.25	0.35
848	Fra	NEU	0.375	0.56	2,500	Fra	ERM	0.275	0.39
874	Fra	MAT	0.35	0.52	2,550	Fra	ERM	0.25	0.35
900	Fra	MAT	0.375	0.56	2,550	Fra	ERM	0.25	0.35
900	Fra	MAT	0.35	0.52	2,582	Fra	ERM	0.25	0.35
925.5	Fra	MAT	0.35	0.52	2,601	Fra	ERM	0.25	0.35
949	Fra	MAT	0.375	0.56	2,621	Fra	ERM	0.25	0.35
1,001	Fra	NEU	0.35	0.52	2,650	Fra	BIE	0.2	0.27
1,050	Fra	MAT	0.35	0.52	2,672	Fra	BOU	0.2	0.27
1,050	Fra	MAT	0.33	0.49	2,700	Fra	BOU	0.225	0.31
1,100	Fra	NEU	0.35	0.52	2,702	Fra	BOU	0.2	0.27
1,151	Fra	NEU	0.35	0.52	2,750	Fra	BOU	0.2	0.27
1,199	Fra	BOU	0.35	0.52	2,799	Fra	BOU	0.2	0.27
1,203	Fra	BOU	0.3	0.44	2,850	Fra	BOU	0.25	0.35
1,250	Fra	BOU	0.3	0.44	2,850	Fra	BOU	0.2	0.27
1,301	Fra	BOU	0.325	0.48	2,900	Fra	NEU	0.225	0.31
1,349	Fra	BOU	0.3	0.44	2,946	Fra	BOU[b]	0.25	0.35
1,349	Fra	BOU	0.35	0.52	2,954	Fra	NEU	0.2	0.27
1,376	Fra	BOU	0.325	0.48	3,003	Fra	NEU	0.225	0.31
1,401	Fra	BOU	0.35	0.52	3,054	Fra	NIS	0.175	0.22
1,425	Fra	NEU[b]	0.3	0.44	3,100	Giv	FRO	0.175	0.22
1,450	Fra	BOU	0.3	0.44	3,150	Giv	FRO	0.2	0.27
1,501	Fra	NEU	0.3	0.44	3,205	Giv	FRO	0.2	0.27

[a] KI (Lille), illite Kübler index (°Δ2θ) before calibration; KIS, Kübler index standard; Fra, Frasnian; Fam, Famennian; Giv, Givetian. Formation and member names are FRO, Fromelennes Formation; NIS, Nismes Formation; ERM, Ermitage Member; BIE, Bieumont Member; BOU, Boussu-en-Fagne Member; NEU, Neuville Formation; MAT, Matagne Formation; FAME, Famenne Formation (Boulvain and Coen-Aubert 1997)

[b] Illite KI values of formation sections are incorporated into that of nearby formation sections due to their small thickness

whereas micrite $\delta^{18}O$ display a larger range from −4.394 to −10.736‰ (Table 3).

The $\delta^{18}O$ values (73 micrites and 43 brachiopods) of the Focant borehole are listed in Table 4 and drawn as two depth distribution figures with formation labels (Fig. 5). As seen with the KI data, the $\delta^{18}O$ distributions of both micrites and brachiopods display a boundary at about −1,200 m dividing the profile into two zones. The micrite values (Fig. 5) of the upper zone range from −4.3 to −12.1‰, without difference between the Matagne and Neuville formations (Upper Frasnian). Their $\delta^{18}O$ range is similar to those of the Lower-Middle Frasnian in the La Boverie quarry. The $\delta^{18}O$ of the lower zone, including the Neuville, Boussu, Bieumont and Ermitage formations (or members), presents a lighter and narrower field varying between −8.0 and −12.3‰. The brachiopod $\delta^{18}O$ (Fig. 5) of the upper zone of the borehole shows a distribution from −4.7 to −9.4‰, similar to that of the La Boverie

Table 3 $\delta^{18}O$ values (‰ PDB) of the brachiopods and of the micrites in the Boverie quarry

Sample no.	Formation or member	$\delta^{18}O$ (PDB) brachiopod	$\delta^{18}O$ (PDB) micrite	Sample no.	Formation or member	$\delta^{18}O$ (PDB) brachiopod	$\delta^{18}O$ (PDB) micrite
B83	Uppermost Boussu	−6.341	−8.956	B40s	Upper Ermitage	−8.380	
f14	Upper Boussu	−7.327	−5.619	B38m	Upper Ermitage		−8.145
f13	Upper Boussu	−5.172	−5.247	B29	Upper Ermitage	−5.793	−6.580
f12	Upper Boussu	−5.383		B26	Upper Ermitage	−7.376	
f12a	Upper Boussu		−4.394	f8	Upper Ermitage	−4.647	−5.055
B120(99)	Upper Boussu	−5.112	−10.736	f7	Middle Ermitage	−5.472	−7.066
B40cO	Upper Ermitage		−8.260				

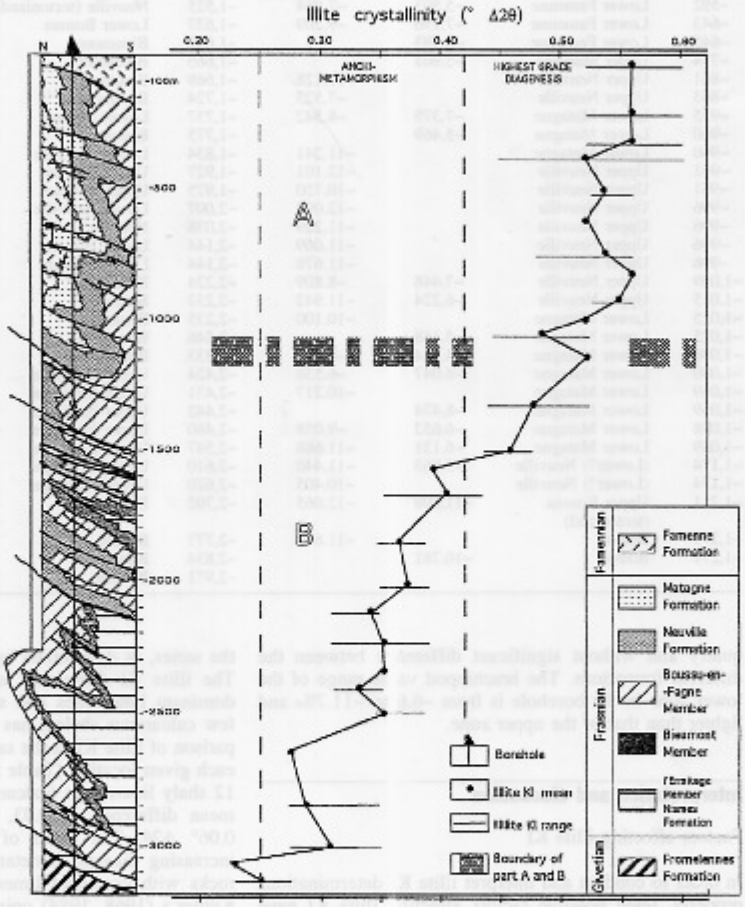

Fig. 4 Frasnian illite KI distributions of the Focant borehole. The KI values of the upper zone (zone *A*) show no significant difference with regional stratigraphical formation and depth based on both mean and range, all belonging to the highest-grade diagenetic zone. The lower zone (zone *B*) displays a clear KI depth gradient within anchizone against structurally repeated Frasnian formations and members. The stratigraphical subdivision and structural analysis of the borehole are from Boulvain and Coen-Aubert (1997) and Lacquement (2001)

Table 4 $\delta^{18}O$ values (‰ PDB) of the brachiopods and of the micrites in the Focant borehole

Depth (m)	Formation or member	$\delta^{18}O$ (PDB) brachiopod	$\delta^{18}O$ (PDB) micrite	Depth (m)	Formation or member	$\delta^{18}O$ (PDB) brachiopod	$\delta^{18}O$ (PDB) micrite
−47.5	Famenne	−9.425	−9.240	−1,290	Boussu		−10.714
−124	Upper Neuville		−11.579	−1,346	Boussu	−10.930	−10.916
−170	Upper Neuville	−5.522	−4.301	−1,373	Boussu	−10.347	−11.493
−196.5	Upper Neuville	−5.098	−5.905	−1,377	Boussu		−9.660
−237	Upper Neuville	−5.179	−9.139	−1,383	Boussu		−11.931
−342	Lower Matagne	−4.703	−9.179	−1,393	Boussu	−7.282	−11.097
−408	Upper Neuville		−11.062	−1,395	Boussu		−10.311
−435	Neuville		−9.943	−1,401	Boussu	−10.931	−11.314
−460	Lower Matagne	−8.504		−1,471	Lower Neuville		−10.820
−477	Lower Matagne	−9.147	−6.854	−1,491	Lower Neuville		−10.523
−490	Lower Matagne		−7.080	−1,522	Neuville (tectonized)		−8.039
−592	Lower Famenne	−5.503	−7.984	−1,525	Neuville (tectonized)	−6.698	−10.422
−643	Lower Famenne	−7.196	−9.209	−1,637	Lower Boussu	−9.079	−11.505
−645	Lower Famenne	−6.593		−1,662	Bleumont	−10.321	−10.244
−714	Upper Matagne	−5.961		−1,665	Bleumont	−10.916	−11.279
−861	Upper Neuville		−11.128	−1,669	Bleumont		−11.624
−863	Upper Neuville		−7.523	−1,724	Bleumont		−11.452
−955	Lower Matagne	−7.375	−8.542	−1,757	Lower Boussu		−10.822
−960	Lower Matagne	−5.469		−1,775	Boussu		−11.703
−960	Lower Matagne		−11.241	−1,834	Lower Neuville		−10.895
−961	Upper Neuville		−12.101	−1,927	Upper Boussu	−6.591	−12.307
−981	Upper Neuville		−10.750	−1,975	Upper Boussu		−11.791
−996	Upper Neuville		−12.093	−2,007	Lower Neuville		−10.978
−996	Upper Neuville		−11.229	−2,038	Neuville		−11.421
−996	Upper Neuville		−11.069	−2,144	Lower Boussu	−9.802	
−996	Upper Neuville		−11.678	−2,144	Lower Boussu		−11.464
−1,009	Upper Neuville	−7.448	−8.809	−2,224	Bleumont		−11.636
−1,015	Upper Neuville	−6.224	−11.942	−2,233	Bleumont	−11.697	
−1,025	Lower Matagne		−10.100	−2,235	Bleumont	−10.744	−10.784
−1,025	Lower Matagne	−5.168		−2,246	Bleumont	−10.517	−11.460
−1,030	Lower Matagne	−4.824	−7.973	−2,333	Boussu inf.	−10.649	−9.644
−1,040	Lower Matagne	−8.047	−6.538	−2,424	Upper Ermitage	−9.254	−11.821
−1,069	Lower Matagne		−10.217	−2,431	Upper Ermitage	−10.904	−11.369
−1,069	Lower Matagne	−8.474		−2,442	Upper Ermitage	−11.638	−9.542
−1,088	Lower Matagne	−6.652	−9.058	−2,460	Upper Ermitage		−11.554
−1,089	Lower Matagne	−6.131	−11.688	−2,547	Upper Ermitage		−9.529
−1,174	(Lower?) Neuville	−5.963	−11.440	−2,610	Upper Ermitage		−11.920
−1,174	(Lower?) Neuville		−10.405	−2,620	Upper Ermitage		−10.456
−1,211	Upper Boussu (tectonized)	−11.698	−12.065	−2,702	Boussu		−10.431
−1,279	Boussu		−11.644	−2,777	Boussu	−10.700	−12.138
−1,279	Boussu	−10.781		−2,834	Boussu	−10.969	
				−2,971	Boussu		−10.726

quarry and without significant difference between the different formations. The brachiopod value range of the lower zone in the borehole is from −6.6 to −11.7‰ and lighter than that of the upper zone.

Interpretation and discussion

Factors affecting illite KI

In order to conduct and interpret illite KI determinations properly, three possible factors affecting illite KI have been evaluated. Temperature has been considered as the most important factor in the study area in our previous works, since the widespread illite KI stratigraphical gradient in the Dinant Synclinorium (Han et al. 2000) is consistent with the temperature increasing with the age of the series, as determined by CAI values (Helsen 1995a). The illite KI difference induced by lithology between dominant limestones and shaly limestones (including a few calcareous shales) has been investigated. The comparison of illite KI in the same formation (or member) at each given location (Table 5) between 31 limestones and 12 shaly limestones (calcareous shales) displays a slight mean difference of 0.03, with a range from 0.01 to 0.06° $\Delta 2\theta$. The trend of decreasing difference with increasing diagenetic/metamorphic grade in the studied rocks with dominant limestones seems consistent with Kübler's (1968, 1984) opinion that gradually weakened lithological influence on KI from diagenesis towards metamorphism becomes negligible at the onset of the anchizone. Considering that limestones are dominant, and their KI mean difference between using and not using shaly limestones is less than 0.01° $\Delta 2\theta$ (see right column

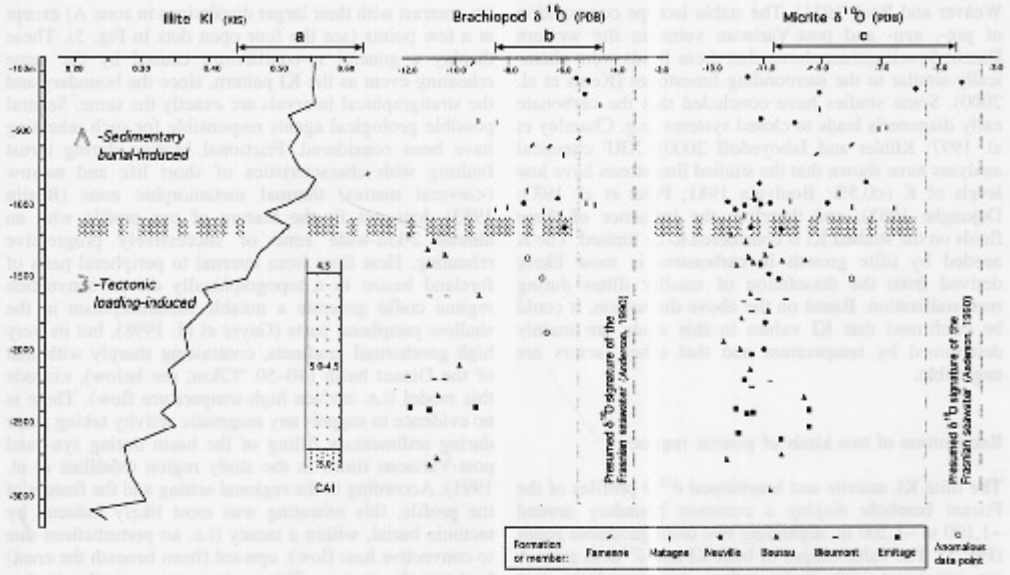

Fig. 5 Illite KI (° $\Delta 2\theta$), micrite and brachiopod $\delta^{18}O$ (PDB) profiles, with part of conodont colour alteration index (CAI) profile (from Helsen 1995b) of the Focant borehole. The three line segments (*a*–*c*) on the tops of the profiles each represent the value ranges of the corresponding surface Frasnian strata at the nearby southern border (*a*) and Boverie quarry (*b*, *c*) of the Dinant Synclinorium, which are used to compare with those of the borehole. Based on these patterns, two geothermal regimes, i.e. sedimentary burial (*A*) and tectonic loading (*B*), are recognised. See text for details

Table 5 Comparison of illite KI values (°$\Delta 2\theta$) between limestones and shaly limestones (including a few calcareous shales)

Location	Formation (or member)	KI limestone (L)	KI shaly limestone (SL)	Lithological difference (SL–L)	Difference (formation–L)
Pry	PHV	0.37 (n=9)[a] 0.33–0.39	0.36 (n=1)	−0.01	−0.001
Soulme	NEU (or VAL)	0.41 (n=3) 0.39–0.43	0.42 (n=3) 0.41–0.45	0.01	0.005
Hautmont	NEU	0.52 (n=3) 0.48–0.58	0.58 (n=2) 0.57–0.58	0.06	0.024
Cerfontaine	PHV	0.52 (n=12) 0.41–0.55	0.57 (n=2) 0.52–0.62	0.05	0.007
Foisches	NEU (or VAL)	0.55 (n=2) 0.52–0.57	0.59 (n=2) 0.57–0.60	0.04	0.02
East Gimnee	BIE	0.56 (n=2) 0.52–0.60	0.58 (n=2) 0.57–0.58	0.02	0.01

[a] n, sample number. Illite KI values in columns of limestones and shaly limestones consist of mean and range. KI value of formation is the mean of all samples (limestones and shaly limestones) in the formation. For the name of formation (or member), see Table 1

of Table 5), the lithology effect is therefore negligible in this study. The stress factor is not yet clear, due to the existence of contrasting conclusions derived from some other studies (Frey 1987). For this reason, an investigation on the relationship between illite KI distribution and structural location has been performed in a single fold (outcrop scale) in the Avesnes quarry (western Dinant Synclinorium) and two thrust faults, one at Villers-le-Gambon (site 6 on Fig. 3) and the other at Franchimont (site 7 on Fig. 3, and Han 1999). As a result, there is no convincing evidence to support the influence of stress, since KI values between the anticline hinge zone and the limb are almost the same, and those in the fault belts seem to be more subject to the stratigraphy, and not the distance to the thrust fault. Increasing K content in the fluids, leading to improved illite KI, has been suggested (e.g.

Weaver and Beck 1971). The stable isotope composition of pre-, syn- and post-Variscan veins in the western Dinant Synclinorium shows that these fluids were chemically similar to the surrounding limestones (Kenis et al. 2000). Some studies have concluded that the carbonate early diagenesis leads to closed systems (e.g. Chamley et al. 1997; Kübler and Jaboyedoff 2000). XRF chemical analyses have shown that the studied limestones have low levels of K (<0.5%; Boulvain 1981; Préat et al. 1983; Dejonghe 1985), and therefore the influence of these fluids on the studied KI is considered to be limited. The K needed by illite growth in carbonates is most likely derived from the dissolution of smaller illites during recrystallization. Based on the above discussion, it could be confirmed that KI values in this study are mainly determined by temperature and that other factors are negligible.

Recognition of two kinds of genetic regimes

The illite KI, micrite and brachiopod $\delta^{18}O$ profiles of the Focant borehole display a common boundary around −1,100 to −1,200 m, separating two distinguishable zones (Fig. 5). The value ranges of both KI and $\delta^{18}O$ in zone A are consistent with their surface correspondents (see Fig. 5, line segments a-c), showing the same values among the formations. The value range of Frasnian KI in zone A, falling into the highest-grade diagenetic zone (i.e. 0.42–0.62° $\Delta 2\theta$ in Han et al. 2000), coincides with the general Devonian stratigraphical illite KI gradient in the southern border of the Dinant Synclinorium (Han et al. 2000, their Fig. 5a). This type of gradient, widely existing in the synclinorium (Dandois 1985; Fielitz and Mansy 1999; Han et al. 2000), is one of the criteria used to recognise a sedimentary burial metamorphism (Merriman and Frey 1999). K–Ar illite ages of 326±7 Ma (Piqué et al. 1984) for the Devonian rocks in the southern border support also the nature of this metamorphism predating the Variscan orogeny which started from Westphalian times in the study area (Fielitz and Mansy 1999). The average $\delta^{18}O$ composition of brachiopods, originally in isotopic equilibrium with seawater (Veizer et al. 1997), is 3.0‰ lighter than the $\delta^{18}O$ signature of the Frasnian seawater (Hurley and Lohmann 1989; Anderson 1990), and the $\delta^{18}O$ micrite values are 4.5‰ lighter than the seawater signature. Based on these KI and $\delta^{18}O$ patterns, it appears that zone A, together with nearby, surface Frasnian strata, experienced a diagenetic modification through the sedimentary burial regime, and kept this record.

Below 1,200 m, a clear KI depth gradient in the Variscan thickened profile, independent of stratigraphy (Fig. 5), indicates an important reheating. This is also confirmed by the conodont colour alteration index (Helsen 1995b), which parallels this gradient (Fig. 5). The $\delta^{18}O$ value ranges of both micrites and brachiopods are generally lighter and narrower than their upper correspondents, and concentrate between −10 and −12‰ (in contrast with their larger dispersions in zone A) except at a few points (see the four open dots in Fig. 5). These display a general re-equilibrium caused by the same reheating event as the KI pattern, since the boundary and the stratigraphical intervals are exactly the same. Several possible geological agents responsible for such reheating have been considered. Frictional heating during thrust faulting with characteristics of short life and narrow (<several metres) thermal metamorphic zone (Bustin 1983) does not fit the feature of our profile with an almost 2-km-wide zone of successively progressive reheating. Heat flow from internal to peripheral parts of foreland basins in a topographically driven convection regime could generate a notable metamorphism in the shallow peripheral parts (Gayer et al. 1998), but its very high geothermal gradients, contrasting sharply with that of the Dinant basin (40–50 °C/km, see below), exclude this model (i.e. surface high-temperature flow). There is no evidence to support any magmatic activity taking place during sedimentary filling of the basin during syn- and post-Variscan times in the study region (Meilliez et al. 1991). According to the regional setting and the feature of the profile, this reheating was most likely induced by tectonic burial, within a steady (i.e. no perturbations due to convective heat flow), upward (from beneath the crust) heat transfer regime. This regime seems similar to that suggested for the Ruhr basin in the northern part of the Variscan belt (western Germany) during maximum burial (Littke et al. 1994; Büker et al. 1995).

The four anomalous data points (open dots in Fig. 5) near the boundary, three in brachiopods and one in micrite, are likely to be the remainders of the sedimentary burial genesis. In this context, these particular brachiopods display a higher resistance to heat-induced isotopic exchange than the micrites, as also noted in zone A where brachiopods are nearer to the original $\delta^{18}O$ seawater value than the micrites. Nevertheless, these minor points do not affect the general pattern of re-equilibration.

Zone B, with a thickness of about 2 km, belongs to the anchizone with its small upper part in the highest grade of diagenesis (Fig. 4). The CAI data of this section (Fig. 5) cannot be used for the temperature estimation of the anchizone, since the same temperature estimated from the CAI zone (4.5–5.0) covers more than 1 km, and complete data below and above this zone are not available. The chlorite KI in the carbonate rocks of the upper Palaeozoic in the study region is not as good as illite KI for recording a depth gradient induced by burial (Han et al. 2000). Therefore, the temperature estimation here is based on the KI zonation alone. If 225–300 °C is adopted as a temperature range for the anchizone (based on Kisch (1987), from 200–250 °C onset to 300 °C high-grade boundary), and approximately represents that of zone B, it could produce a small $\delta^{18}O$ difference (2–3‰) between the uppermost and the lowermost parts in an isotopically homogeneous fluid, using the calcite–water oxygen-fractionation equation (Faure 1986, Table 2.5.1). The studies on carbonate textures and geochemistry of Upper

Palaeozoic sequences, and particularly in the Devonian beds of the Dinant Synclinorium, and adjacent areas have shown that these series attained a closed state soon after early diagenetic cementation. This is based on isotopic similarities between fluids and surrounding limestones in both pre-Variscan and Variscan times (Weis and Préat 1994; Chamley et al. 1997; Kenis et al. 2000). So, no important fluid invasion (there is no important dolomitization, no non-carbonate veins, etc.) is to be expected, and the trapped fluids produced quite homogeneous oxygen values derived from an isotopically similar composition of limestones. As a result, the observed $\delta^{18}O$ profile of zone B is probably formed by tectonic reheating in such 'carbonate closed systems', with unimportant isotopic fractionation difference.

The profile through zone B (Fig. 5) also reveals the different responses of illite KI, CAI and $\delta^{18}O$ in the depth interval of 2 km to the anchimetamorphic conditions. The KI profile, which generally increases in metamorphic grade with depth (hence, temperature), demonstrates a detailed and very sensitive gradient. By contrast, no CAI change with depth can be detected within the CAI 4.5–5.0 interval (more than 1 km thick) compared with the KI data, although the complete CAI profile does show a similar gradient. The $\delta^{18}O$ values of both brachiopods and micrites show re-equilibration but without a depth trend. These comparative results show that illite KI analysis is more sensitive than CAI, and more appropriate than oxygen isotopes to highlight a progressive burial metamorphism.

Reheating and Variscan thrusting

Using the CAI data, Helsen (1995a) has estimated that the ultimate sedimentary burial depth of the basal Frasnian in the southern border of the Dinant Synclinorium was around 4,000 m (Fig. 6a). At this depth, Frasnian illite KI reached their temperature maximum as a sedimentary burial genesis, and the original $\delta^{18}O$ signature of seawater in Frasnian carbonates was mostly erased during this burial diagenesis. Subsequent Variscan deformation by thrusting and folding placed these Frasnian strata at various depths during the tectonism (Fig. 6b). In such a profile, the heat suffered by the Frasnian in zone B could be significantly higher than their previously experienced sedimentary burial heat, while the upper zone (A) did not encounter higher heat than during the previous regime. The reason is that these zones were at different depth-related temperature locations in the Variscan tectonic profile, with a steady, upward heat transfer. Between both zones must lie a boundary where the tectonic loading heat approximately equals previous burial heat. Above this boundary, sedimentary burial-genetic illite KI and diagenetically modified $\delta^{18}O$ would remain unchanged. Below the boundary, the second heating on the Frasnian series started during the largest Variscan tectonic loading, and thus illite KI suffered re-improvement to become tectonic loading-genetic KI (KIt) and form the depth gradient. Meanwhile, diagenetic $\delta^{18}O$ in both micrites and brachiopods re-equilibrated with fluids in a closed system. It is obvious that the location of such a boundary for other stratigraphical series in this tectonic loading profile could vary, and must be deeper for older strata in the above-assumed heat transfer regime.

The A/B boundary is an important indicator in such a tectonic loading profile and represents the isothermal location of two regimes experienced by the Frasnian series. This knowledge is useful to recover the dimension of ultimate Variscan tectonic stacking.

Based on the illite KI gradient of zone B and its comparison with the KI/depth curves with the geothermal gradient from USA Gulf Coast shales, the palaeogeothermal gradient of a tectonic loading regime can be estimated. The thickness interval spanned by the KI range (0.30 and 0.50° 2θ) of zone B is about 1,500 m, according to its calculated average slope of 0.013° 2θ/100 m (see above). These values can be placed on KI versus depth curves with different geothermal gradients resulting from computer modelling of the USA Gulf Coast shales (Merriman in Han et al. 2000, their Fig. 10b) and can be checked for each curve. The result shows that the KI range of our zone B (0.30–0.50° 2θ) and its thickness interval are consistent with a geothermal gradient of 40 °C/km. This estimated gradient of the tectonic loading regime corresponds to that of the sedimentary burial regime in the Dinant basin (Han et al. 2000), which has been based on KI slope, CAI temperature and comparison with the same Gulf Coast curves. The equality of deduced palaeogeothermal gradients between both regimes can also be seen from the thermal history of the adjacent northern Variscan front zone (Kenis et al. 2000), although in this case, 50 °C/km is deduced from fluid inclusions of quartz.

Since there is no significant difference of the geothermal gradients between these regimes in the study area, the isothermal character of the boundary could be simply represented by an iso-depth (i.e. tectonic loading depth of the boundary=Frasnian sedimentary burial depth). Thus, the sedimentary burial depth of Frasnian beds can be used to determine the original tectonic loading depth of the boundary (Fig. 6b). The recovered tectonic loading depth of the boundary is equivalent to about 4,000 m, since no significant sedimentation took place in the study region after Variscan thrusting (Meilliez and Mansy 1990). From this, it is estimated that the thickness of the removed thrust sheet in the southern border of the Dinant Synclinorium around the Focant borehole is about 3,000 m.

Comparison of illite KI patterns with other orogenic belts

Two stages of thermal development (i.e. sedimentary burial and subsequent tectonic stacking) are commonly experienced in basins at the periphery of many orogenic belts. In the external domain of the southern Canadian Appalachians, illite KI data of Lower Palaeozoic series

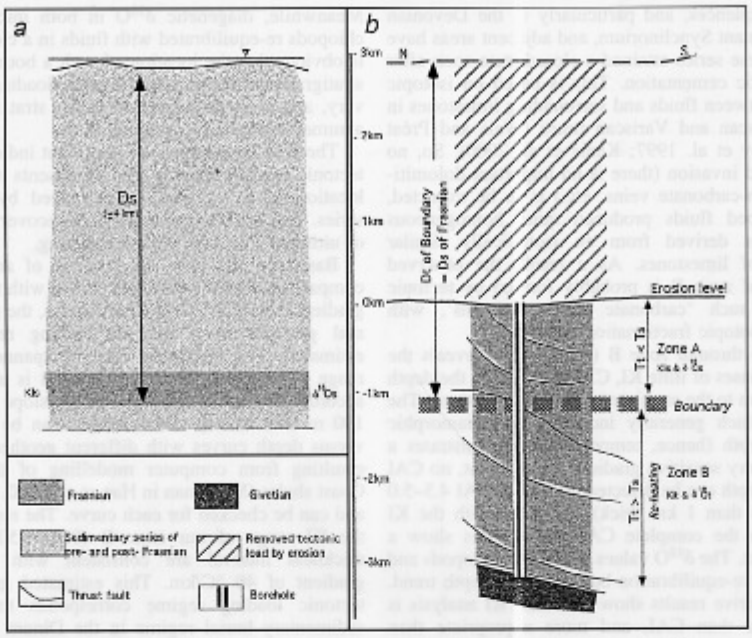

Fig. 6a, b The two recognised geothermal regimes and tentative recovery of the restoration Variscan tectonic load. **a** Frasnian sedimentary burial depth (*Ds*) at the end (early Namurian times) of basinal sedimentation is about 4,000 m in the southern border (Helsen 1995a), and genesis of sedimentary burial illite KI (*KIs*). The $\delta^{18}O$ signature of carbonate components was lighter ($\delta^{18}Os$) during diagenesis. *b* The Frasnian series were repeated at varying depths by subsequent Variscan movements. The comparison between sedimentary burial heat (*Ts*) and tectonic loading heat (*Tt*) the Frasnian suffered could differentiate two zones. In the upper zone (zone A), the heat (*Tt*) is lower than that of the previous regime due to less tectonic burden. Therefore, their sedimentary burial genetic recorders (*KIs* and $\delta^{18}Os$) are unchanged. The reheating appeared in the lower zone (zone B) due to significantly higher heat than the previous regime, which has re-improved illite KI (*KIt*) and re-equilibrated the isotopic signature ($\delta^{18}Ot$). The boundary indicates a location where *Tt* equals *Ts*. Since the geothermal gradients of the two regimes are equivalent (see text), the tectonic loading depth (*Dt*) of the boundary is equal to the sedimentary burial depth (*Ds*) of the Frasnian in the southern border. So, it could be deduced that the boundary bore about 4,000 m of tectonic load, and the load removed by subsequent erosion is near 3,000 m

(Yang and Hesse 1991) display an inverted metamorphic pattern, i.e. more mature, older rocks tectonically overlie less mature, younger rocks. This inverted pattern also appears in other orogenic belts, such as in the main central thrust zone of the central Nepal Himalayas (Jamieson et al. 1996), in the Glarus Alps (Frey 1988), and in the Variscan thrust front in northern France (Bouquillon et al. 1985). Such patterns did not develop in situ and are generally the result of tectonic assembly by thrust faults juxtaposing deep buried strata over less-buried strata. Their metamorphism existed prior to the thrusting, even though local modification of the pattern may be syn- or post-tectonic (Merriman and Frey 1999). Likewise, symmetrical repetition of the KI values caused by folding (Dandois 1985) and metamorphic hiatuses resulting from thrust faulting (Merriman and Frey 1999) are also the result of post-metamorphic tectonic displacement. An accretionary burial pattern comprises a sequence of continuous metamorphic zones developed in situ and shows grade increasing into younger tracts of strata within the thrust stack (Merriman and Frey 1999). In the Focant profile, this stratigraphy-related trend of in-situ metamorphism (younger tracts of strata downwards) does not appear. Based on the preceding comparison and discussion, two types of very low-grade metamorphisms at the periphery of orogenic belts can be recognised. One is pre-orogenic burial metamorphism, and is subsequently tectonically displaced to develop varied illite KI patterns, such as inverted stacking, hiatuses and so on. This type frequently keeps a basin-wide stratigraphic gradient (i.e. increasing metamorphic grade with stratigraphic age). The other is an in-situ syn- or post-orogenic tectonic loading metamorphism (during maximum stacking) and parallels the depth gradient in the fold-thrust stack.

Conclusions

The illite KI and $\delta^{18}O$ (including CAI) patterns of the tectonically repeated Frasnian carbonates of the Focant borehole at the periphery of the northern Variscan belt (Belgium, France) document an in-situ reheating due to Variscan thickened load following sedimentary burial. It is typically characterized by depth gradient illite KI (CAI) and re-equilibrated $\delta^{18}O$ being more mature and lighter respectively than their sedimentary burial-genetic precursors.

The boundary between the tectonic loading reheated lower zone and the sedimentary burial-genetic upper zone of the Focant profile is an important thermal indicator. It represents a special location for the Frasnian stage in the Variscan fold-thrust stack where the tectonic loading heat which the Frasnian strata suffered should equal the sedimentary burial heat it had previously experienced. Based on this knowledge and the relevant geological setting, the thickness of the eroded thrust sheet around the Focant borehole is estimated to be around 3,000 m.

Two periods of oxygen isotopic exchanges taking place in the brachiopods and micrites occurred, initially during the highest-grade diagenesis and then during the anchimetamorphism. They caused $\delta^{18}O$ records of these carbonate components to become increasingly lighter than the presumed Frasnian seawater signature, although brachiopods present a higher resistance to heat-induced isotopic exchange than the micrites. The comparison among illite KI, CAI and $\delta^{18}O$ profiles of the Focant borehole indicates that illite KI analysis is more sensitive than CAI, and more appropriate than $\delta^{18}O$ in highlighting a progressive, very low-grade metamorphism in the burial of the basins.

Acknowledgements Grateful acknowledgement is expressed to Prof. H. Chamley (Université de Lille) for his support and encouragement in the process of forming the main opinions appearing in this paper. Thanks are presented to Prof. J.F. Deconinck (Université de Rennes) for helpful discussion on clay minerals, to Mr. D. Malengros, and Ph. Recourt (University of Lille) for X-ray diffractometry analysis. We also thank the reviewers Drs. R.O. Greiling, L.N. Warr and V. Wrede (Ruprecht Karls University), and an anonymous reviewer for constructive comments. Thanks are due to Dr. M. Coen-Aubert, Dr. J. Godefroid and Prof. P. Bultynck (Institut royal des Sciences Naturelles de Belgique), Dr. M. Bertrand (Université de Bruxelles) and Dr. X. Devleeschouwer (Service géologique de Belgique) for help during sampling and collecting data, Mrs. J.E. Cartlidge (University of Oxford) for the mass spectrometry measurements, and Mr. G. Bernardinis (Université de Bruxelles) for the preparation of thin sections. The investigations were in part supported by the Wiener-Anspach Foundation, the British Council Funds, and by the Communauté française de Belgique (Tournesol project n°02/046).

References

Adams R, Vandenberghe N (1993) The Meuse Valley cross section reconsidered. In: Mulock-Houwer JA, Pilaar WF, Van de Graaff-Trouwboest T (eds) Ardennes, Belgium: architecture of a Paleozoic carbonate ramp and platform, field trip 1. AAPG Int Conf and Exhibit, The Hague, pp 15–18

Anderson TF (1990) Temperature from oxygen isotope ratios. In: Briggs DEG, Crowther PR (eds) Palaeobiology: a synthesis. Blackwell, Oxford, pp 403–406

Bless MJM (1983) Late Devonian and Carboniferous ostracode assemblages and their relationship to the depositional environment. Bull Soc Belg Géol 92:31–53

Bless MJM, Bouckaert J, Paproth E (1989) The Dinant nappes: a model of tensional listric faulting inverted into a compressional folding and thrusting. Bull Soc Belg Géol 98:221–230

Boulvain F (1981) Sédimentologie et géochimie de la Formation de Trois-Fontaines (Givétien) à Vaucelles (Bord Sud du Synclinorium de Dinant). Mém fin études, Université de Bruxelles

Boulvain F, Coen-Aubert M (1997) Le sondage de Focant: lithostratigraphie et implications structurales. Ministère des Affaires Economiques, Bruxelles, Mem Geol Surv Belg 43

Boulvain F, Coen M, Coen-Aubert M, Bultynck P, Casier JG, Dejonghe L, Tourneur F (1993) Les formations frasniennes du massif de Philippeville. Ministère des Affaires Economiques, Bruxelles, Prof Pap 259

Boulvain F, Bultynck P, Casier JG, Coen M, Coen-Aubert M, Dejonghe L, Dumoulin V, Ghysel P, Godefroid J, Helsen S, Lacroix D, Laloux M, Mouravieff N-A, Sartenaer P, Tourneur F, Vanguestaine M (1999) Les formations du Frasnien de la Belgique. Ministère des Affaires Economiques, Bruxelles, Mem Belg Geol Surv 43

Bouquillon A, Chamley H, Debrabant P, Piqué A (1985) Etude minéralogique et géochimique des forages de Jeumont et Epinoy (Paléozoïque du Nord de la France). Ann Soc Géol Nord 104:167–179

Brindley GW, Brown G (1980) Crystal Structures of clay minerals and their X-ray identification. Mineral Soc Lond

Bliker C, Littke R, Welte DH (1995) 2D-modelling of the thermal evolution of Carboniferous and Devonian sedimentary rocks of the eastern Ruhr Basin and northern Rhenish Massif, Germany. Z Dtsch Geol Ges 146:321–339

Bultynck P, Helsen S, Hayduckiewich J (1998) Conodont succession and biofacies in upper Frasnian formations (Devonian) from the southern and central parts of the Dinant Synclinorium (Belgium)—Timing of facies shifting and correlation with late Frasnian events. Bull Inst R Sci Nat Belg, Sci Terre 68:25–75

Busby CJ, Ingersoll RV (eds) (1995) Tectonics of sedimentary basins. Blackwell, Oxford

Bustin RM (1983) Heating during thrust faulting in the Rocky Mountains: friction or fiction? Tectonophysics 95:309–328

Chamley H, Proust JN, Mansy J-L, Boulvain F (1997) Diagenetic and palaeogeographic significance of clay, carbonate and other sedimentary components in the middle Devonian limestones of western Ardenne, France. Palaeogeogr Palaeoclimatol Palaeoecol 129:369–385

Dandois P (1985) Le métamorphisme des terrains paléozoïques de la partie médio-occidentale de l'Ardenne. PhD Thesis, Université Catholique de Louvain

Dejonghe L (1985) Contribution à l'étude métallogénique du Synclinorium de Verviers (Belgique). PhD Thesis, Université Pierre et Marie Curie, Paris VI, Mém Sci Terre

Einsele G (1992) Sedimentary basins: evolution, facies and sediment budget. Springer, Berlin Heidelberg New York

Faure G (1986) Principles of isotope geology. Wiley, New York

Fielitz W, Mansy J-L (1999) Pre- and synorogenic burial metamorphism in the Ardenne and neighbouring areas (Rhenohercynian zone, Central European Variscides). Tectonophysics 309:227–256

Fortey NJ, Roberts B, Hirons SR (1993) Relationship between metamorphism and structure in the Skiddaw Group, English Lake District. Geol Mag 130:631–638

Frey M (1987) Very low-grade metamorphism of clastic sedimentary rocks. In: Frey M (ed) Low temperature metamorphism. Blackie, Glasgow, pp 9–58

Frey M (1988) Discontinuous inverse metamorphic zonation, Glarus Alps, Switzerland: evidence from illite crystallinity data. Bull Suisse Minéral Pétrogr 68:171–183

Gayer R, Garven G, Rickard D (1998) Fluid migration and coal-rank development in foreland basins. Geology 26:679–682
Goffette O, Liégeois J-P, André L (1991) Age U-Pb sur zircon dévonien moyen à supérieur du magmatisme bimodal du massif de Rocroi (Ardenne, France), implications géodynamiques. C R Acad Sci Paris 312:1155–1161
Goudalier M (1998) Dolomitisation des calcaires du Frasnien moyen en Belgique: contrôles sédimentaire, diagénétique et tectonique. PhD Thesis, Université de Lille I
Han G (1999) Paleozoic clay mineral sedimentation and diagenesis in the Dinant and Avesnes Basins (Belgium, France): relationship with Variscan tectonism. PhD Thesis, Université Libre de Bruxelles
Han G, Préat A, Charnley H, Deconinck J-F, Mansy J-L (2000) Paleozoic clay mineral sedimentation and diagenesis in the Dinant and Avesnes Basins (Belgium, France): relationship with Variscan tectonism. Sediment Geol 136:217–238
Helsen S (1995a) Burial history of Palaeozoic strata in Belgium as revealed by conodont colour alteration data and thickness distributions. Geol Rundsch 84:738–747
Helsen S (1995b) Burial history of Palaeozoic strata in Belgium and adjacent areas based on conodont alteration data. PhD Thesis, Katholieke Universiteit Leuven
Holser WT, Magaritz M, Ripperdan RL (1996) Global isotopic events. In: Walliser OH (ed) Global events and event stratigraphy in the Phanerozoic. Springer, Berlin Heidelberg New York, pp 63–88
Holtzapffel T (1985) Les minéraux argileux. Préparation. Analyse diffractométrique. Soc Géol Nord Publ 12
Hurley HF, Lohmann KC (1989) Diagenesis of Devonian reefal carbonates in the Oscar range, Canning Basin, Western Australia. J Sediment Petrol 44:837–861
Jamieson RA, Beaumont C, Hamilton J, Fullsack P (1996) Tectonic assembly of inverted metamorphic sequences. Geology 24:839–842
Juch D (2000) Eine neue Deutung syntektonischer Inkohlungskomponenten des Ruhrkarbons. Glückauf-Forschungsh 61(1):27–34
Kasimi R, Préat A (1996) Sédimentation de rampe mixte silico-carbonatée des couches de transition eifélienne-givétiennes franco-belges. Deuxième partie: cyclostratigraphie et paléostructuration. Bull Centres Rech Explor-Prod Elf-Aquitaine 20:61–90
Kenis I, Muchez PH, Sintubin M, Mansy JL, Lacquement F (2000) The use of a combined structural, stable isotope and fluid inclusion study to constrain the kinematic history at the northern Variscan front zone (Bettrechies, northern France). J Struct Geol 22:589–602
Kisch HJ (1987) Correlation between indicators of very low-grade metamorphism. In: Frey M (ed) Low temperature metamorphism. Blackie, Glasgow, pp 227–300
Kisch HJ (1990) Calibration of the anchizone: a critical comparison of illite 'crystallinity' scales used for definition. J Metamorph Geol 8:31–46
Kübler B (1967a) La cristallinité de l'illite et les zones tout à fait supérieures du métamorphisme: étages tectoniques. Coll Neuchâtel 1966, pp 105–121
Kübler B (1967b) Anchimétamorphisme et schistosité. Bull Centres Rech Explor-Prod Elf-Aquitaine 1:259–278
Kübler B (1968) Evaluation quantitative du métamorphisme par la cristallinité de l'illite. Bull Centres Rech Explor-Prod Elf-Aquitaine 2:385–397
Kübler B (1984) Les indicateurs des transformations physiques et chimiques dans la diagenèse, température et calorimétrie. In: Lagache M (ed) Thémométrie et barométrie géologiques. Soc Franç Minéral Cristallogr, Paris, pp 489–596
Kübler B, Jaboyedoff M (2000) Illite crystallinity. Earth Planet Sci 331:75–89
Lacquement F (2001) L'Ardenne Varisque. Déformation progressive d'un prisme sédimentaire pré-structuré, de l'affleurement au modèle de chaîne. Soc Géol Nord 29
Littke R, Büker C, Lückge A, Sachsenhofer RF, Welte DH (1994) A new evaluation of paleoheatflows and eroded thicknesses for the Carboniferous Ruhr Basin, Western Germany. Int J Coal Geol 26:155–183
Machel GH, Cavell PA, Patey KS (1996) Isotopic evidence for carbonate cementation and recrystallization, and for tectonic expulsion of fluids into the Western Canada sedimentary basin. Geol Soc Am Bull 108:1108–1119
Mamet B, Préat A (1996) Geology of Belgium. In: Moores EM, Fairbridge RW (eds) Encyclopedia of Earth Sciences Series, European and Asian regional geology. Chapman & Hall, London, pp 78–83
Mansy JL, Meilliez F (1993) Eléments d'analyse structurale à partir d'exemples pris en Ardenne-Avesnois. Ann Soc Géol Nord 93:45–60
Mansy JL, Lacquement F, Meilliez F, Hanot F, Everaerts M (1997) Interprétation d'un profil sismique pétrolier sur le méridien de Valenciennes (Nord de la France). Aardk Mededel 8:127–129
Marshall JD (1992) Climatic and oceanographic isotopic signals from the carbonate rock record and their preservation. Geol Mag 129:143–160
Meilliez F, Mansy J-L (1990) Déformation pelliculaire différenciée dans une série lithologique hétérogène: le Dévono-Carbonifère de l'Ardenne. Bull Soc Géol Fr 8:177–188
Meilliez F, André L, Blieck A, Fielietz W, Goffette O, Hance L, Khatir A, Mansy JL, Overlau P, Verniers X (1991) Ardenne-Brabant. Sci Geol Bull 44:3-29
Merriman RJ, Frey M (1999) Patterns of very low-grade metamorphism in metapelitic rocks. In: Frey M, Robinson D (eds) Low-grade metamorphism. Blackwell, Oxford, pp 61–107
Merriman RJ, Roberts B, Peacor DR (1990) A transmission electron microscope study of white mica crystallite size distribution in a mudstone to slate transitional sequence, North Wales, UK. Contrib Mineral Petrol 106:27–40
Merriman RJ, Pharaoh TC, Woodcock NH, Daly P (1993) The metamorphic history of the concealed Caledonides of Eastern England and their foreland. Geol Mag 130:613–620
Merriman RJ, Roberts B, Peacor DR, Hirons SR (1995) Strain-related differences in the crystal growth of white mica and chlorite: a TEM and XRD study of the development of metapelitic microfabrics in the Southern Uplands thrust terrane, Scotland. J Metamorph Geol 13:559–576
Michot P (1976) Le segment varisque et son antécédent calédonien. In: Beiträge zur Kenntnis der Europäischen Varisziden. Franz Kossmat Symp 1974, Nova Acta Leopoldina, Abth Dtsch Naturforsch, Leopoldina Neue Folge 45, 224:201–228
Moore DM, Reynolds RC (1989) X-ray diffraction and the identification and analysis of clay minerals. Oxford University Press, Oxford
Muchez P, Boven J, Bouckaert J, Leplat P, Viaene W, Wolf M (1991) Illite crystallinity in the Carboniferous of the Campine-Brabant basin (Belgium) and its relationship to organic maturity indicators. N Jb Geol Paläontol Abh 182:177–181
Nieto F, Sanchez-Navas A (1994) A comparative XRD and TEM study of the physical meaning of the white mica "crystallinity" index. Eur J Mineral 6:611–621
Paproth E, Dusar M, Verkaeren P, Bless MJM (1994) Stratigraphy and cyclic nature of Lower Westphalian deposits in the boreholes KB174 and KB206 in the Belgian Campine. Ann Soc Géol Belg 117:169–189
Piqué A, Huon S, Clauer N (1984) La schistosité hercynienne et le métamorphisme associé dans la vallée de la Meuse, entre Charleville-Mézières et Namur (Ardennes franco-belges). Bull Soc Belg Géol 93:55–70
Préat A, Cauet S, Herbosch A (1983) Caractère épigénétique étranger des Gîtes Filoniens Pb-Zn (Ba-F) du District du Synclinorium de Dinant (Belgique). Miner Deposita 18:349–363
Raoult JF, Meilliez F (1986) Commentaires sur une coupe structurale de l'Ardenne selon le méridien de Dinant. Ann Soc Géol Nord 105:97–109
Reynolds R C (1980) Interstratified clay minerals. In: Brindley GW, Brown G (eds) Crystal structures of clay minerals and their X-ray identification. Mineral Soc Lond, pp 249–303

Robinson D, Merriman RJ (1999) Low-temperature metamorphism: an overview. In: Frey M, Robinson D (eds) Low-grade metamorphism. Blackwell, Oxford, pp 1–9

Robinson D, Warr LN, Bevins RE (1990) The illite crystallinity technique: a critical appraisal of precision. J Metamorph Geol 8:333–344

Robion P, Averbach O, Sintubin M (1999) Fabric development and metamorphic evolution of the Palaeozoic slaty rocks from the Rocroi Massif (French-Belgian Ardennes): new constraints from magnetic fabrics, phyllosilicate preferred orientation and illite crystallinity data. Tectonophysics 309:257–273

Schaer JP, Persoz F (1976) Aspects structuraux et pétrographiques du Haut-Atlas calcaire de Midelt (Maroc). Bull Soc Géol Fr 18:1239–1250

Sharp ZD (1999) Application of stable isotope geochemistry to low-grade metamorphic rocks. In: Frey M, Robinson D (eds) Low-grade metamorphism. Blackwell, Oxford, pp 227–260

Smellie JL, Roberts B, Hirons SR (1996) Very low- and low-grade metamorphism in the Trinity Peninsula Group (Permo-Triassic) of northern Graham Land, Antarctic Peninsula. Geol Mag 133:583–594

Teichmüller M, Teichmüller R, Weber K (1979) Inkohlung und Illit-Kristallinität, vergleichende Untersuchungen im Mesozoikum und Paläozoikum von Westfalen. Fortschr Geol Rheinld Westf 27:201–276

Thorez J, Goemare E, Dreesen R (1988) Tide-and wave-influenced depositional environments in the Psammites du Condroz (Upper Famennian) in Belgium. In: Boer PL De, Van Gelder A, Nio SD (eds) Tide-influenced sedimentary environments and facies, sedimentology and petroleum geology. Reidel, Dordrecht, pp 389–415

Veizer J, Bruckschen P, Pawellek F, Diener A, Podlaha OG, Carden GAF, Jasper T, Korte C, Strauss H, Azmy K, Ala D (1997) Oxygen isotope evolution of Phanerozoic seawater. Palaeogeogr Palaeoclimatol Palaeoecol 132:159–172

Warr LN (1996) Standardized clay mineral crystallinity data from the very low-grade metamorphic facies rocks of southern New Zealand. Eur J Mineral 8:115–127

Warr LN, Rice AHN (1994) Interlaboratory standardization and calibration of clay mineral crystallinity and crystallite size data. J Metamorph Geol 12:141–152

Warr LN, Primmer TJ, Robinson D (1991) Variscan very low-grade metamorphism in southwest England: a diastathermal and thrust-related origin. J Metamorph Geol 9:751–764

Warr LN, Greiling RD, Zachrisson E (1996) Thrust-related very low grade metamorphism in the marginal part of an orogenic wedge, Scandinavian Caledonides. Tectonics 15:1213–1229

Weaver CE, Beck KC (1971) Clay water diagenesis during burial: how mud becomes gneiss. Geol Soc Am Spec Pap 134

Weis D, Préat A (1994) Variations du niveau marin dans le Dévonien carbonaté de Belgique: approches géochimiques et isotopiques (Sr, C et O) (deuxième partie). Bull Soc Géol Fr 165:485–497

Yang C, Hesse R (1991) Clay minerals as indicators of diagenetic and anchimetamorphic grade in an overthrust belt, external domain of southern Canadian Appalachians. Clay Miner 26:211–231

Ziegler PA (1990) Geological atlas of western and central Europe. Shell Int Petroleum Maatschappij BV